Supporting Information for:

$Cu_{2-x}S$/PbS Core/Shell Nanocrystals with Improved Chemical Stability

Patrick Y. Yee[¥,*], Sarah Brittman[¥], Nadeemullah A. Mahadik[¥], Joseph G. Tischler[¥], Rhonda M. Stroud[¥], Alexander L. Efros[¥], Peter C. Sercel[§], Janice E. Boercker[¥]

[¥]U.S. Naval Research Laboratory, 4555 Overlook Avenue SW, Washington D.C. 20375, United States

[§]Department of Applied Physics and Materials Science, California Institute of Technology, Pasadena, 91125, California, United States

*Email: patrick.yee.ctr@nrl.navy.mil

Materials and Methods

Materials. Oleic acid (90%), 1-octadecene (90%), lead oxide (99.999%), bis(trimethylsilyl)sulfide (synthesis grade), copper (II) acetylacetonate (≥99.9% trace metals basis), dioctyl ether (99%), 1-dodceanethiol (≥98%), hexane (anhydrous 95%), ethanol (anhydrous ≥99.5%), toluene (anhydrous 99.8%) and acetonitrile (anhydrous 99.8%), were all purchased from Sigma Aldrich. Unless specified below, all chemicals were used as received without further purification. Flasks were heated using a heating mantle and temperature controller (J-KEM Scientific Apollo dual temperature controller).

Pb Oleate Synthesis. Lead oxide and oleic acid were mixed and heated to 100 °C under vacuum for ~1-2 hour. The oleic acid to lead oxide mole ratio used was 3:1. The solution started as a yellow cloudy solution and gradually became clear and colorless. Once clear and colorless with no further bubbles forming under vacuum, the flask was back-filled with argon, cooled slightly, and poured into centrifuge tubes. It is important to pour the mixture while it is still warm, because if it is allowed to cool to room temperature in the flask, then it will become solid and be difficult to remove from the flask. The mixture in the centrifuge tubes was left in air overnight, lightly capped, and allowed to cool to room temperature and solidify. The solid was then washed with acetone in order to remove any unreacted oleic acid. Acetone was added to each tube and the solid was broken up to suspend in the acetone, followed by centrifuging at 6000 rpm for 1 minute. The clear supernatant was discarded and the process was repeated for a total of 5 washes. The powdery white solid was then transferred to glass vials and put in a vacuum oven at room temperature and 2.5 torr for at least 12 hours. The oven was then back filled with argon and the Pb oleate in the glass vials was stored and used in a glovebox. The yield was around 80%.

$Cu_{2-x}S$ Core Reaction. The $Cu_{2-x}S$ nanocrystals were synthesized according to the method of Turo and MacDonald,[1] with slight modifications to the heating temperature and reaction time. 0.2719 g of copper (II) acetylacetonate was combined with 5 mL of dodecanethiol and diluted, while stirring (750 rpm), with 45 mL of dioctyl ether in a 100 mL, three-necked, round-bottom flask. The flask was then put under vacuum for 30 minutes at room temperature and afterward switched to argon flow. To avoid degassing uncontrollably, the vacuum line must be opened to the flask very gradually, without initial stirring, as the polar solvents contain a lot of water. Under argon, the mixture was heated (initial rate ~ 7 °C/minute to 160 °C and then ~1.3 °C/minute to 200 °C, although the second ramp was asymptotic rather than linear) to 200 °C by using the "300 mL – 2 mL" setting (equivalent to a variac setting of 50%) on the temperature controller. While the temperature ramped, the mixture's color gradually changed from a turbid light blue to a cloudy white/yellow, to transparent yellow, orange, red, and finally brown. At 199 °C, the mixture turned black and was reacted for an additional 60 minutes, starting at the color change to black. After 60 minutes, the flask was removed from heat and allowed to cool, while stirring, to room temperature for about 40 minutes. The mixture was then transferred into a N_2 glovebox, and split into four centrifuge tubes. 12 mL of anhydrous ethanol was added to each tube and subsequently centrifuged at 6000 rpm for 5 minutes. After the supernatant was decanted, each precipitate was resuspended in 0.5 mL of chloroform and mixed with 20 mL of anhydrous ethanol, which was centrifuged at 6000 rpm for 2 minutes. The supernatant was again decanted and all of the resulting $Cu_{2-x}S$ cores from both tubes were suspended in 12 mL of anhydrous hexane. This was stored for one to two days in the glovebox, over which time a light-brown, waxy, precipitate settled at the bottom of the vial. The supernatant was then decanted into a centrifuge tube and centrifuged at 6000 rpm for 2 minutes to remove any excess precipitate. We identified this precipitate, via XRD, as the Cu alkanethiolate $CuSC_{12}H_{25}$, (**Figure S1**).[2] The remaining, cleaned $Cu_{2-x}S$ was dried completely and was resuspended in hexane to create a 10.6 mg/ml solution.

X-ray diffraction confirming byproduct in $Cu_{2-x}S$ nanocrystal synthesis

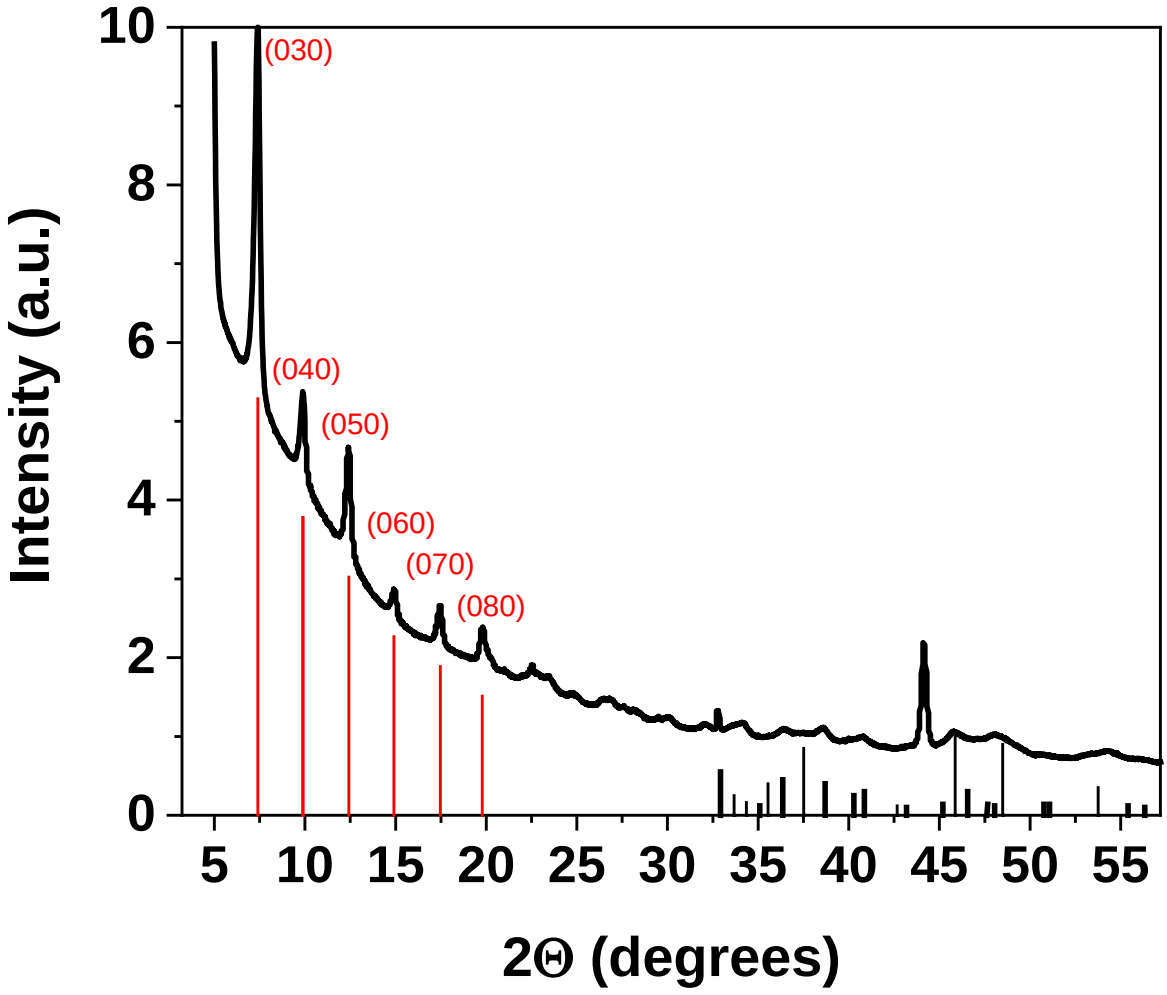

Figure S1: X-ray diffraction of the Cu alkanethiolate byproduct removed from the $Cu_{2-x}S$ core nanocrystals during the cleaning process. The red vertical lines are representative of the alkyl-alkyl spacing for $CuSC_{12}H_{25}$, which has a d-spacing of about 3.5 Å. The black stick patterns are representative of monoclinic chalcocite $Cu_{2-x}S$ (PDF# 00-023-0096).

We note that the Cu alkanethiolate is not fully isolated from the $Cu_{2-x}S$ cores as we still see lattice spacings for $Cu_{2-x}S$ at higher 2Θ (black stick pattern).

Calculation for a N monolayer thick PbS shell

As stated in the Experimental Section of the main text, the definition of a monolayer (ML) is taken as an additional layer of Pb or S atoms added to the surface and is estimated as a diameter change of 5.932 Å, or the (100) d-spacing of rocksalt PbS. The initial core volume is calculated based on the starting $Cu_{2-x}S$ core diameter (5.9 nm). The shell volume is then calculated by accounting for the increased monolayer thickness from PbS, which in turn is used to calculate the amount of moles of PbS needed. Note that that Pb oleate to bis(trimethylsilyl)sulfide) ratio must be 1.5 to keep the product soluble. An example calculation can be seen for a N=4 monolayer thick PbS shell in **Table S1**.

Core or Core/Shell Diameter nm	Cu_2S Core or Core/Shell Vol 1 NX nm^3	ML Thickness (200) of PbS nm	Shell RXN Number (ML X)	Shell Volume nm^3	Weight Cu_2S g	total Volume Cu_2S nm^3	Number Cu_2S NX	Tot PbS Shell Vol nm^3	g PbS needed	Moles PbS needed for ML X
5.9	107.5361	0.2966	1	35.806	0.0106	1.89E+18	1.76E+16	6.302E+17	0.0047	2.00E-05
6.4932	143.3424	0.2966	2	42.984	0.0106	1.89E+18	1.76E+16	7.566E+17	0.0057	2.40E-05
7.0864	186.3269	0.2966	3	50.818	0.0106	1.89E+18	1.76E+16	8.945E+17	0.006	2.89E-05
7.6796	237.1452	0.2966	4	59.307	0.0106	1.89E+18	1.76E+16	1.043E+18	0.007	3.31E-05

Total moles Pb and S needed 4ML (sum of purple column)	g Pb oleate 1.5X	mL of .57 M (TMS)2S
0.00010561	0.122001302	0.185280776

Table S1. Example calculation showing the total number of moles of PbS needed to add a theoretical 4 ML of PbS shell to a $Cu_{2-x}S$ core.

For a 10 ML shell reaction, 0.98 g of Pb oleate was mixed with 17.5 mL of 1-octadecene. This mixture was heated to 60 °C and 2 mL of the $Cu_{2-x}S$ nanocrystal solution in hexane and 1.5 mL of the 0.57 M bis(trimethylsilyl)sulfide stock solution, both at room temperature, were injected simultaneously.

For a 15 ML shell reaction, 2.05 g of Pb oleate was mixed with 15.88 mL of 1-octadecene. This mixture was heated to 60 °C and 2 mL of the $Cu_{2-x}S$ solution in hexane and 3.12 mL of the 0.57 M bis(trimethylsilyl)sulfide stock solution, both at room temperature, were injected simultaneously.

The cleaning process for each N shell reaction is the same as stated in the Experimental section of the main text.

Examples of bright-field TEM images used to measure the PbS shell thickness and PbS shell thickness error bar estimation

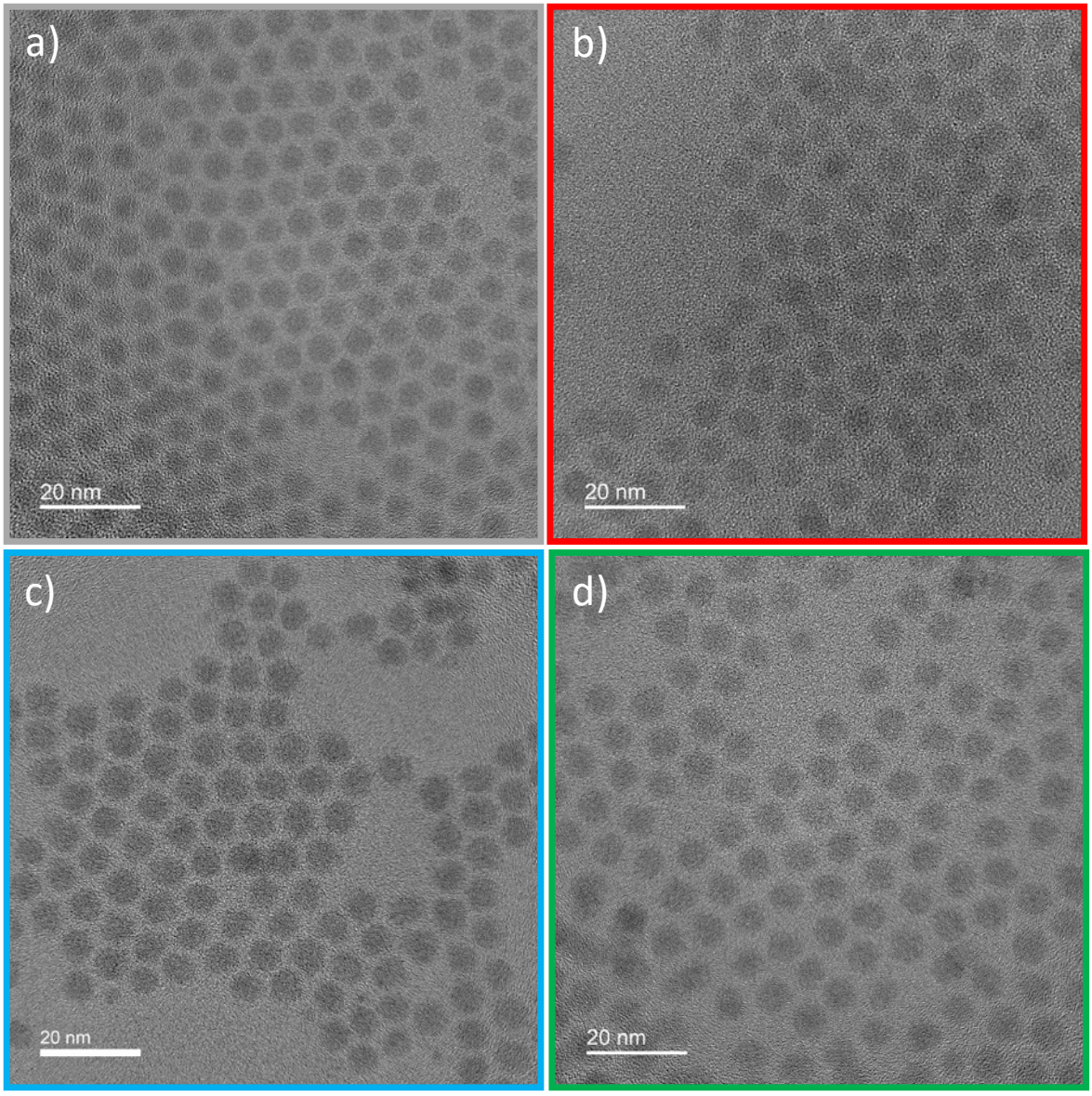

Figure S2. Bright-field TEM images of 6.2 ± 0.4 nm $Cu_{2-x}S$ core nanoparticles (a), 7.4 ± 0.5 nm 4 ML $Cu_{2-x}S$/PbS core/shell nanoparticles (b), 7.2 ± 0.6 nm 10 ML $Cu_{2-x}S$/PbS core/shell nanoparticles (c), and 7.5 ± 0.6 nm 15 ML $Cu_{2-x}S$/PbS core/shell nanoparticles (d). Note that the monolayer thickness is calculated using the respective $Cu_{2-x}S$ cores for each shell reaction.

Bright-field images on a JEOL JEM-2200FS TEM (**Figure S2**) demonstrate the spherical shape of the nanocrystals is maintained upon PbS shell addition. TEM was used to determine the PbS shell thickness. Even though the shell is not seen in the TEM images, the increase in the average nanocrystal diameter can be used to measure the PbS shell thickness. The size histograms of the parent $Cu_{2-x}S$ cores and their respective $Cu_{2-x}S$/PbS core/shell nanoparticles are shown in **Figures 2a-c** of the main text, indicating the deposition of ~1.5 monolayers of PbS (**Figure 2d**).

The error bars for the PbS shell thickness were estimated from the average absolute change in nanocrystal diameter standard deviation upon PbS shell addition (found from bright-field TEM images), which is a measure of the inter-nanocrystal shell non-uniformity. This is because if the PbS shell was 100% uniform on all the particles, then the standard deviation of the nanocrystal size would not change after shell addition and the error bars would be zero. However, if the shell thicknesses are not uniform, which is the case for these core/shell nanocrystals, the standard deviation will change, increasing or decreasing depending on how the shell thickness is distributed to the larger and smaller nanocrystals. Thus the absolute change in standard deviation can be used to estimate the error bars for the PbS shell thickness. This estimation of the PbS shell variation is a measure of the shell non-uniformity between nanocrystals and not the non-uniformity of the shell around a single nanocrystal.

Additional STEM-HAADF images and EDS maps of 15 ML core/shell heterostructures

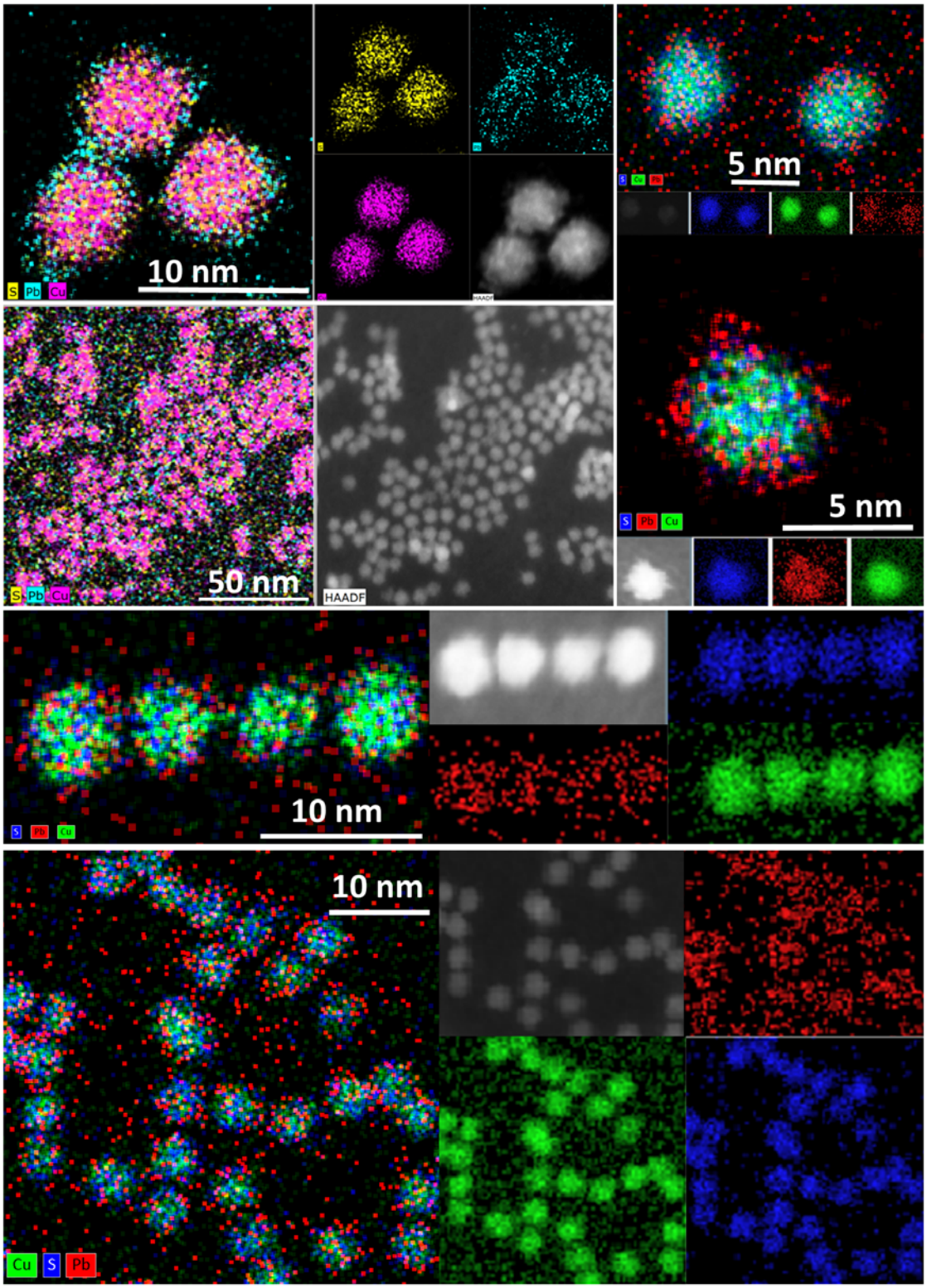

Figure S3. Additional STEM-HAADF images and EDS maps of the patchy PbS shells around the $Cu_{2-x}S$ cores.

HAADF-STEM and EDS map of a $Cu_{2-x}S$/PbS core/shell synthesis with Pb and S concentrations corresponding to 19 ML

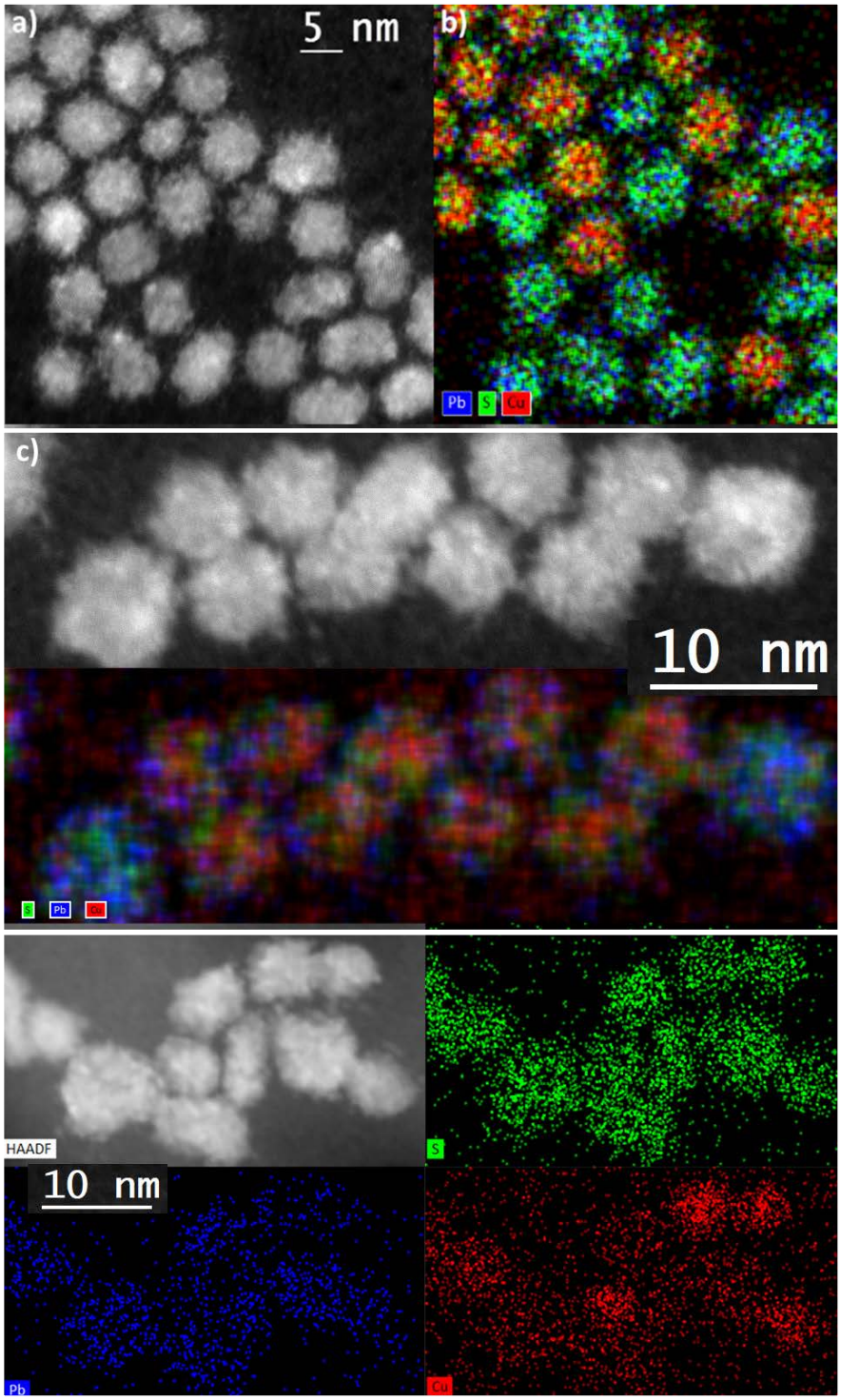

Figure S4. HAADF-STEM image (a), corresponding EDS map (b) shows two particle types - Cu-rich $Cu_{2-x}S$/PbS core/shells (predominantly red) and plain PbS (blue/green) - for a $Cu_{2-x}S$/PbS core/shell nanocrystal synthesis using lead and sulfur concentrations corresponding to 19 ML, and additional HAADF-STEM images and EDS maps (c).

A $Cu_{2-x}S$/PbS core/shell reaction using larger lead and sulfur concentrations (19 ML) than reported in the main text resulted in two populations (**Figure S4**), where there are both copper-rich core/shells (predominantly red) and plain PbS (blue/green). As briefly mentioned in the main text, it has been shown for $Cu_{2-x}Se$ nanocrystals that those nanocrystals with more Cu vacancies will cation exchange more readily than those with fewer vacancies.[3] The djurleite crystal phase of $Cu_{2-x}S$ should therefore cation exchange more readily, as it is more Cu deficient than the low-chalcocite phase. If each individual nanocrystal were a solid-solution composed of both low-chalcocite and djurleite,[4] we would expect this 19 ML shell reaction to result in one population of nanocrystals that have more Pb-rich regions and more Cu-rich regions within the individual nanocrystal. Instead, we see two distinct populations that are either evenly distributed with Cu-rich regions (red) or evenly distributed with Pb-rich regions (blue/green). Thus, we hypothesize that this dual population of nanocrystals resulting from the 19 ML reaction, results from starting with two distinct $Cu_{2-x}S$ compositions where each $Cu_{2-x}S$ nanocrystal is either 100% low-chalcocite or 100% djurleite, rather than having nanocrystals with a solid-solution distribution of both phases.

For a 19 ML shell reaction, 3.28g of Pb oleate was mixed with 14.01 mL of 1-octadecene. This mixture was heated to 60 °C and 2 mL of the $Cu_{2-x}S$ solution in hexane and 4.99 mL of the 0.57 M bis(trimethylsilyl)sulfide stock solution, both at room temperature, were injected simultaneously.

Effect of dielectric environment on surface plasmon energy

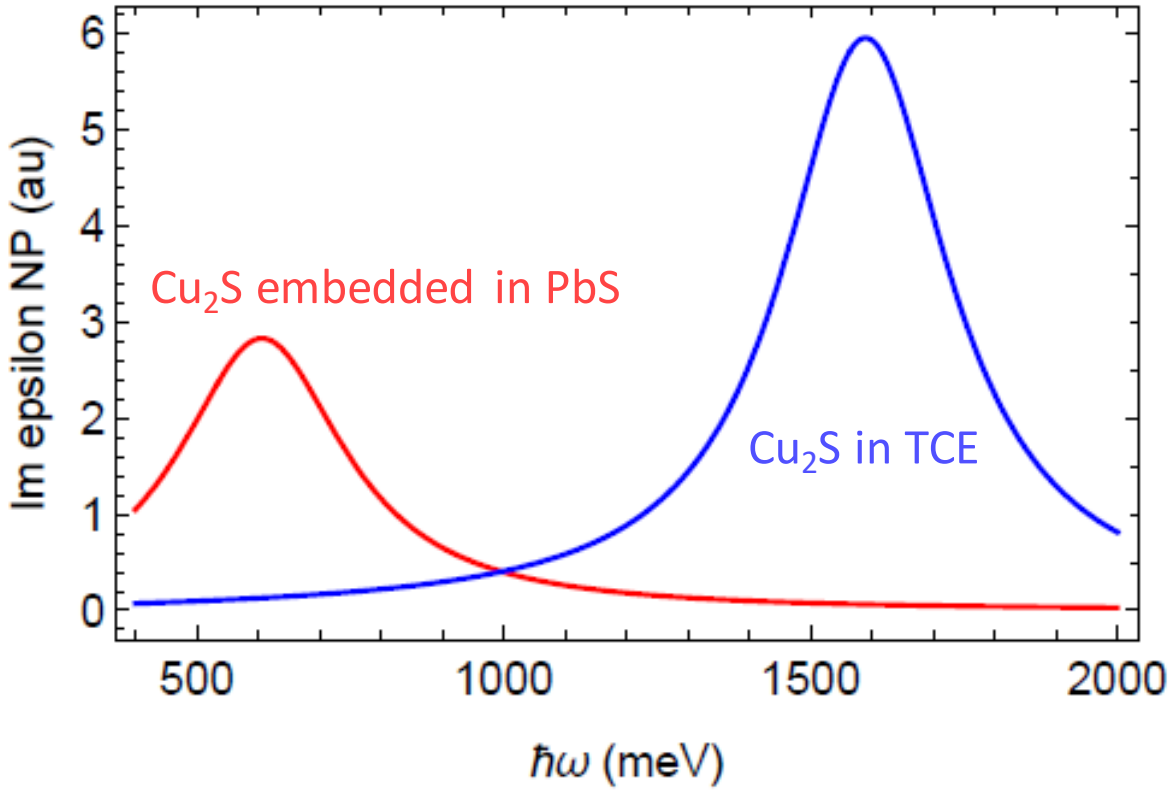

Figure S5. Calculated plasmon resonance for $Cu_{2-x}S$ embedded in a matrix of PbS (red) and $Cu_{2-x}S$ in tetrachloroethylene (TCE) (blue).

An example calculation only accounting for dielectric effects of the environment around our nanocrystals indicates that a redshift would occur upon PbS shell addition, as seen in **Figure S5.** In this calculation, we use the dielectric constants of tetrachloroethylene (2.2), which is the solvent used in absorbance and photoluminescence measurements, and bulk PbS (17) to represent a bare $Cu_{2-x}S$ plasmon and $Cu_{2-x}S$ cores embedded in a matrix of PbS, respectively. The calculation assumed a carrier density of 10^{23} cm^{-3} in the $Cu_{2-x}S$ nanoparticle. This suggests that the blueshift of the plasmon resonance for the core/shell nanoparticles relative to the parent $Cu_{2-x}S$, seen in **Figure 2f** of the main text, must be due to a change in Cu vacancies and carrier density during the phase change from low-chalcocite to djurleite, as opposed to the change in dielectric constant around the $Cu_{2-x}S$ core upon PbS shell deposition.

Surface scattering Drude model of $Cu_{2-x}S$ and $Cu_{2-x}S$/PbS samples to estimate free carrier density

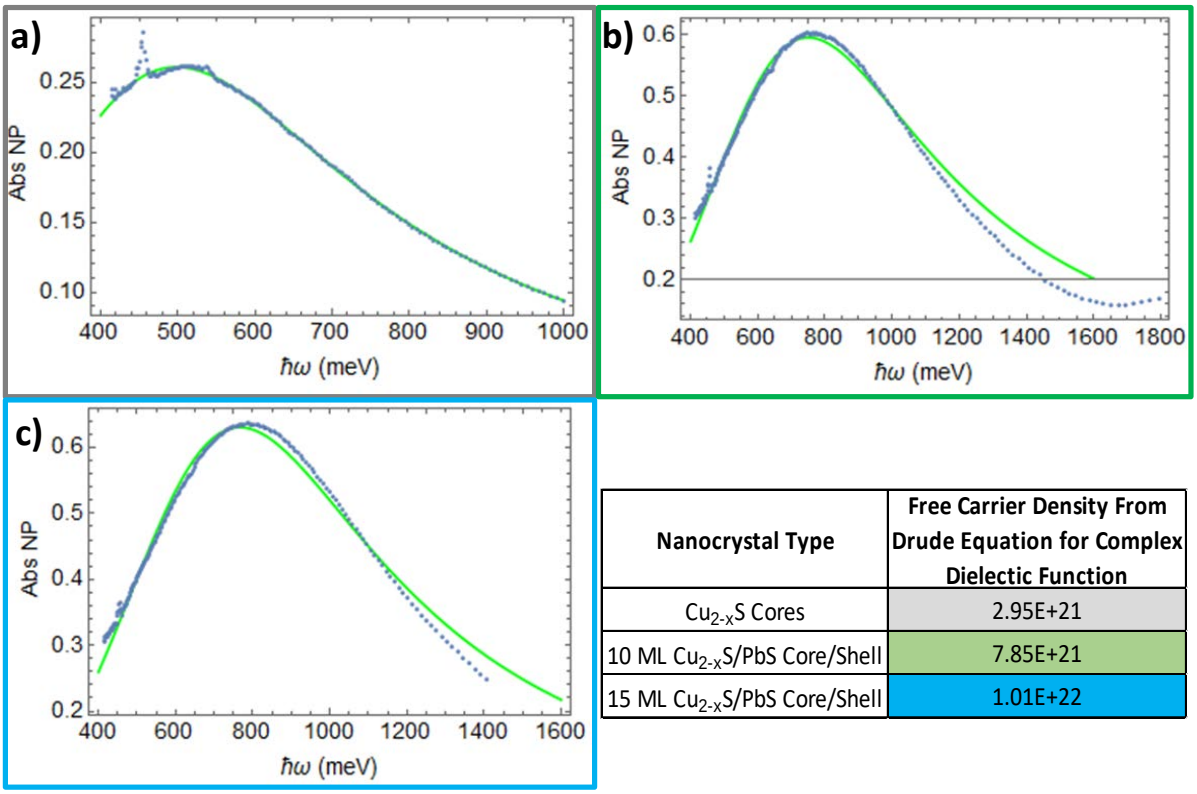

Nanocrystal Type	Free Carrier Density From Drude Equation for Complex Dielectic Function
$Cu_{2-x}S$ Cores	2.95E+21
10 ML $Cu_{2-x}S$/PbS Core/Shell	7.85E+21
15 ML $Cu_{2-x}S$/PbS Core/Shell	1.01E+22

Figure S6: Surface scattering model fits to the absorbance spectra of our $Cu_{2-x}S$ core (a), 10 ML $Cu_{2-x}S$/PbS core/shell (b), and 15 ML $Cu_{2-x}S$/PbS core/shell. The carrier concentrations from these fits are given in the table.

The surface scattering Drude model, in which the surface plasmon damping, **γ**, is taken to be determined by the surface scattering of the free carriers, **γ=1/ t**, with collision time, **t**, proportional to the nanoparticle radius divided by the carrier Fermi velocity, $\mathbf{v_f}$, or $\mathbf{t = A\,R/(v_f)}$, was used to fit the absorbance spectra of our $Cu_{2-x}S$ cores, 10 ML $Cu_{2-x}S$/PbS core/shells, and 15 ML $Cu_{2-x}S$/PbS core/shells shown in **Figure S6**.[5] These fits provide free carrier density estimates for our nanoparticle samples. As briefly discussed in the main text, the Drude model fits show an increase in carrier concentration as the core/shell reaction concentrations increase. This trend is similar to the increase in carrier concentration range expected from the crystal structures predicted from the XRD results (see **Figure 2e** and **Table S2**).

Comparing the carrier density (N) calculated using the Drude model vs. crystal structure vacancies

$Cu_{2-x}S$ Crystal Phase	Free Carrier Density (cm^{-3})	Nanocrystal Type	Free Carrier Density From Drude Equation for Complex Dielectic Function
$Cu_{1.995}S$ low-chalcocite	1.14E+20	$Cu_{2-x}S$ Cores	2.95E+21
$Cu_{1.97}S$ copper rich Djurleite	6.96E+20	10 ML $Cu_{2-x}S$/PbS Core/Shell	7.85E+21
$Cu_{1.94}S$ less copper rich Djurleite	1.40E+21	15 ML $Cu_{2-x}S$/PbS Core/Shell	1.01E+22

Table S2. A table of free carrier density, N (cm^{-3}), calculated from the absorbance spectra of our $Cu_{2-x}S$ and $Cu_{2-x}S$/PbS samples using the Drude model (green) and the expected carrier densities from the possible crystal phases of the $Cu_{2-x}S$ cores (yellow).

The free carrier densities, N (cm^{-3}) are calculated from the fits of the experimental absorbance to the Drude model (**Figure S6**) and are compared to the free carrier densities calculated from the expected $Cu_{2-x}S$ crystal phase, as deduced from the XRD data.

Example calculations for stoichiometric free carrier densities as predicted via the XRD data

Crystal Phase	Core Volume (cm^3)	Unit Cell Volume (nm^3)	Unit Cells Per NX	Vacancies Per Unit Cell	Vacancies Per NX	Free Carrier Density (cm^{-3})
Low-Chalcocite	1.0754E-19	4.39	24.52	0.5	12.3	1.14E+20
$Cu_{1.97}S$ copper rich Djurleite	1.0754E-19	5.74	18.72	4	74.9	6.96E+20
$Cu_{1.94}S$ less copper rich Djuleite	1.0754E-19	5.74	18.72	8	149.8	1.39E+21

Table S3. Example calculations for the free carrier densities according to crystal structure phases as seen in the XRD data.

Table S3 shows the example calculations for these stoichiometric carrier densities, where the core volume is based on the $Cu_{2-x}S$ nanoparticle diameters measured in the bright-field TEM images (**Figure 2** and **Figure S2**). The number of unit cells is calculated as the ratio of the $Cu_{2-x}S$ core volume to the volume of the djurleite and chalcocite unit cells. The number of vacancies per nanocrystal for each phase is based on the number of vacancies per unit cell reported by Sands et al.[4] The stoichiometric free carrier densities are then calculated by dividing the number of vacancies per nanocrystal by the core volume.

Absorbance data of PbS quenching experiment showing that the PbS shell stops the plasmon blueshift of the $Cu_{2-x}S$ cores

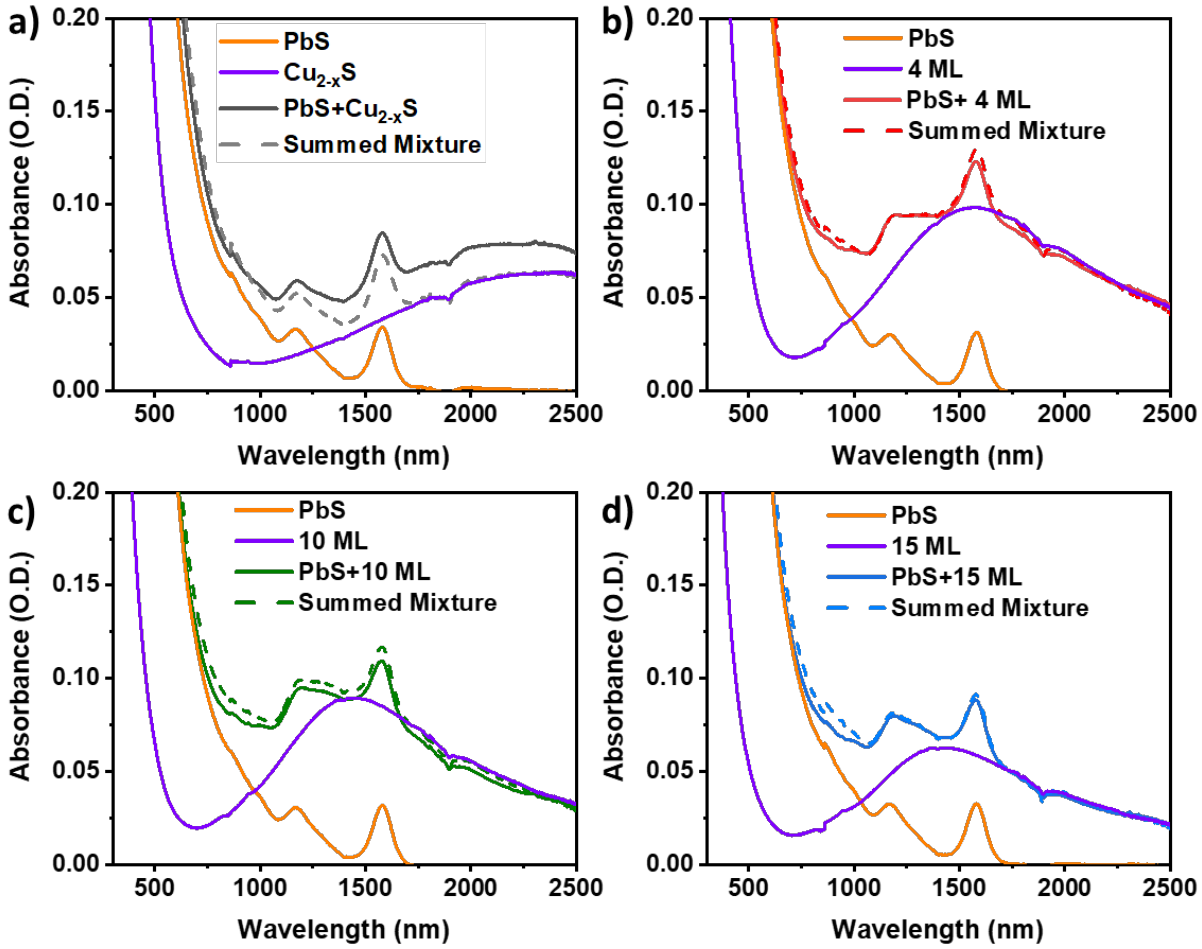

Figure S7. Absorbance spectra of the PbS photoluminescence quenching experiment samples for PbS+$Cu_{2-x}S$ (a), PbS+4 ML (b), PbS+10 ML (c), PbS+15 ML (d). The summed mixtures (dashed lines) are the mathematical sum of the spectra for individual components for each sample set (PbS = orange, $Cu_{2-x}S$ or $Cu_{2-x}S$/PbS = purple).

The absorbance data shown in **Figure S7a** indicates that the $Cu_{2-x}S$ core plasmon is growing stronger and blueshifts when mixed with PbS made using the synthesis reported by Weideman et al.,[6] as the solid grey curve has a higher optical density (O.D.) than the dashed curve, which is the addition of the spectra of the individual components in the sample. In contrast, **Figures S7b-d** show minimal change with the $Cu_{2-x}S$/PbS core/shell plus PbS samples (solid curves) relative to the summed absorbance of the mixtures (dashed curves). In conjunction with the photoluminescence shown in **Figure 3a** of the main text, this indicates that the PbS shell on the core/shell nanoparticles prevents Cu from leaving the $Cu_{2-x}S$ cores to interact with the PbS nanocrystals and quench their photoluminescence.

Absorbance and photoluminescence control experiments confirming Cu atoms quench PbS nanocrystals

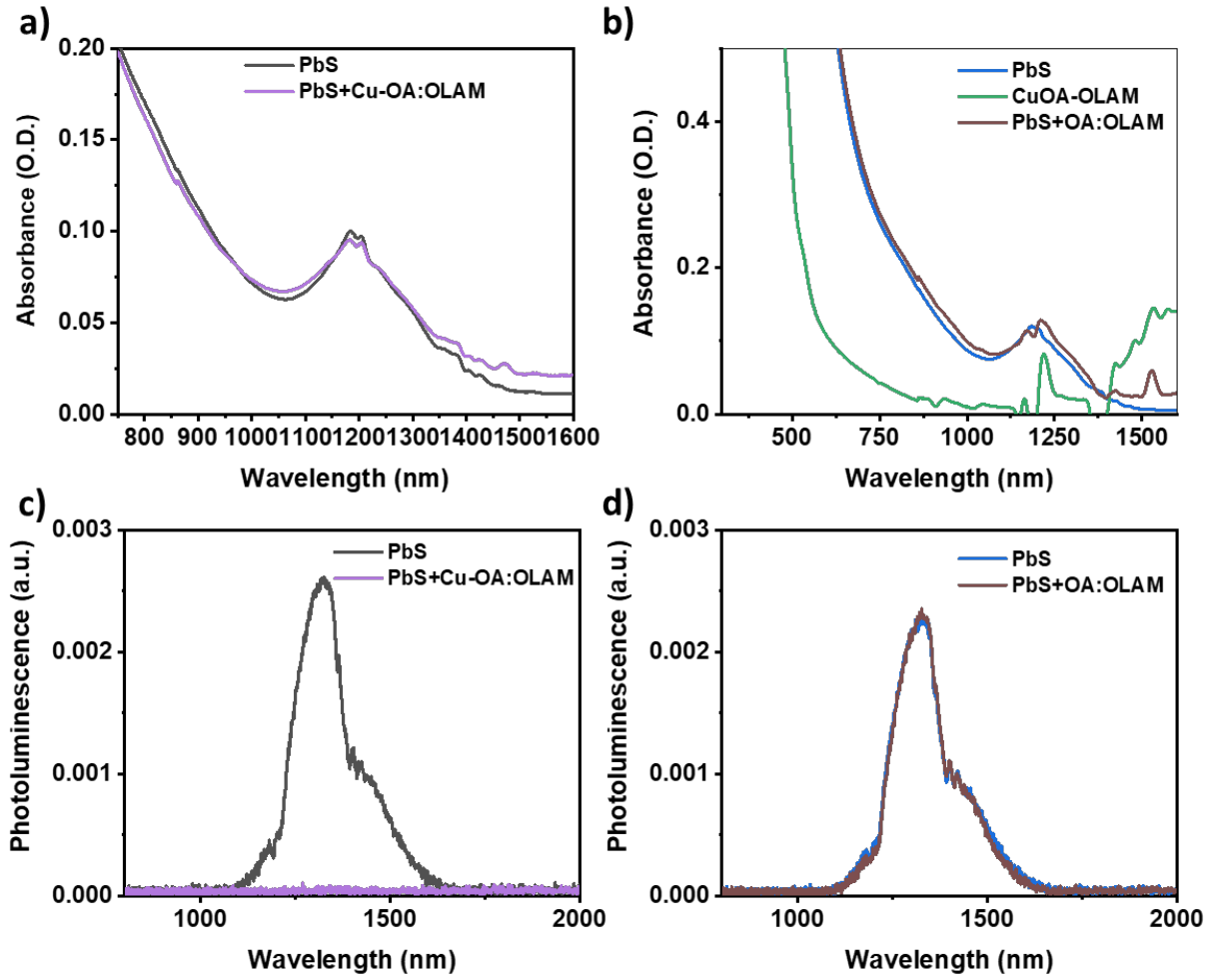

Figure S8. Absorbance spectra of control mixtures in hexane of PbS and Cu-OA:OLAM (a) and PbS and OA:OLAM (b), and photoluminescence spectra of control mixtures of PbS and Cu-OA:OLAM (c) and PbS and OA:OLAM (d)

In order to confirm that the Cu atoms from the $Cu_{2-x}S$ are quenching the photoluminescence of PbS, we show that adding Cu-oleic acid:oleylamine (OA:OLAM) to PbS quenches the PbS photoluminescence, as seen in **Figure S8**. In **Figure S8a**, we show that the PbS absorbance (black) is unchanged with the addition of Cu-OA:OLAM (purple). In Figure **S8b**, we see adding OA:OLAM to PbS nanocrystals does not change their absorbance spectrum notably, and that pure Cu-OA:OLAM does not have a significant amount of absorbance at the emission energy of the PbS nanocrystals. The photoluminescence spectra in **Figures S8c and d** confirm the PbS photoluminescence quenching is due to the Cu atoms (purple) and not from the OA:OLAM mixture (brown) itself. The absorbance and photoluminescence samples prepared in hexane.

Cu-OA:OLAM was synthesized by adding 0.2719g of Cu(II) acetylacetonate into a 50 mL, 3-neck flask with 25 mL of oleic acid and 25 mL of oleylamine. This mixture was pulled under vacuum to remove any H_2O for 1 hour, and heated to 170°C and a change in color from blue to orange was observed. This mixture was then cooled to room temperature and brought into the glovebox.

PbS photoluminescence quenching experiment after being stored as a dry powder for 12 days

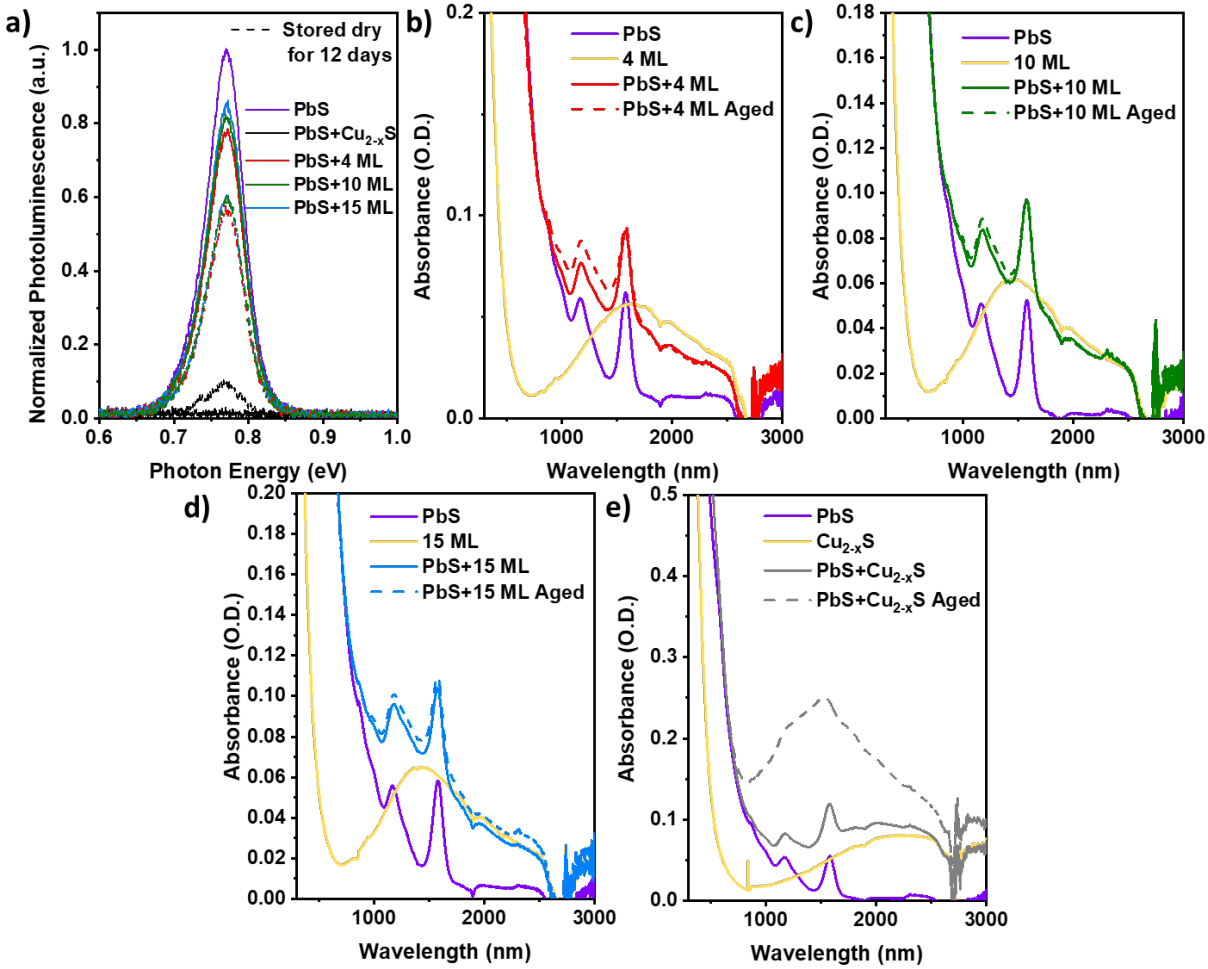

Figure S9. Photoluminescence of mixtures of PbS and either $Cu_{2-x}S$ or the $Cu_{2-x}S$/PbS core/shells after being stored as a dry powder for 12 days (a) and absorbance spectra of these 12 days stored dry samples for PbS+4 ML (b), PbS+10ML (c), PbS+15ML. (d), and PbS+$Cu_{2-x}S$ (e). The solid lines are at t=0 (initial mixture).

As seen in the dashed curves in **Figure S9a**, the PbS photoluminescence still does not completely quench when mixed with the $Cu_{2-x}S$/PbS core/shell nanoparticles after being stored as a dry powder for 12 days. This photoluminescence does decrease, however, indicating that the PbS shell on the $Cu_{2-x}S$/PbS core/shell nanoparticles does not completely prevent Cu atoms from interacting with the PbS nanocrystals. While the PbS photoluminescence does decrease with the core/shell nanoparticles after 12 days, the photoluminescence of the PbS with pure $Cu_{2-x}S$ is now completely quenched after being stored dry for 12 days. This effect is clearly seen in the absorbance of the PbS with $Cu_{2-x}S$/PbS samples (**Figures S9b-d**), where there is no significant effect on the absorbance of the $Cu_{2-x}S$/PbS plasmon after being stored dry. Meanwhile, it is clear that the $Cu_{2-x}S$ plasmon blueshifts and increases in intensity even when stored dry for the PbS+$Cu_{2-x}S$ sample (**Figure S9e**).

PbS photoluminescence quenching experiment after being stored in hexane for 12 days

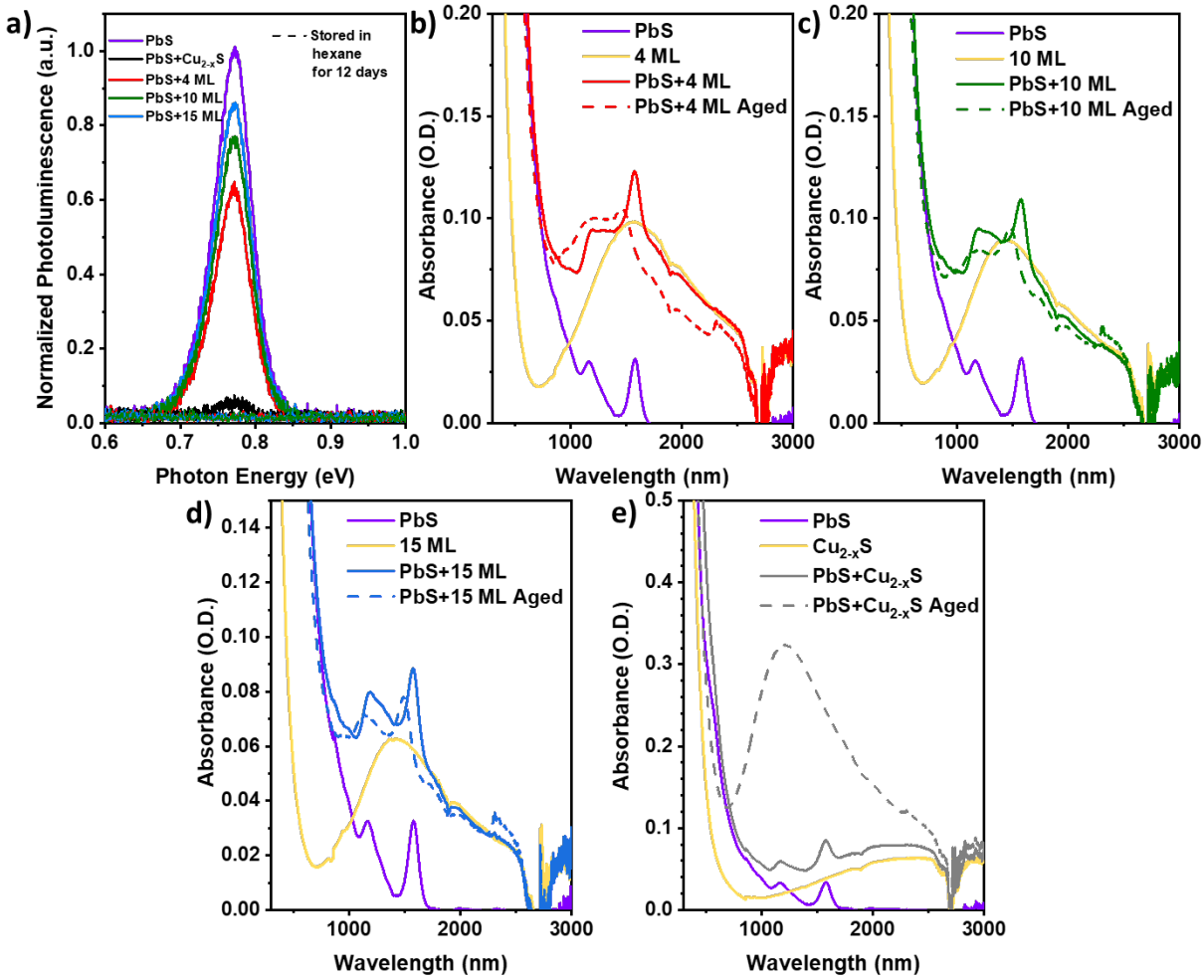

Figure S10. Photoluminescence of mixtures of PbS and either $Cu_{2-x}S$ or the $Cu_{2-x}S$/PbS core/shells after sitting in hexane for 12 days (a) and absorbance spectra of these hexane-stored samples for 12 days PbS+4 ML (b), PbS+10ML (c), PbS+15ML. (d), and PbS+$Cu_{2-x}S$ (e). The solid lines are at t=0 (initial mixture).

As seen in **Figure S10a**, the photoluminescence of the mixed PbS plus either $Cu_{2-x}S$ or $Cu_{2-x}S$/PbS samples after being stored in hexane is completely quenched, despite initially helping prevent the PbS photoluminescence from quenching as seen in **Figure 3a** of the main text. Furthermore, we see in the absorbance spectra in **Figures S10b-d** that while the initial mixtures did not affect the absorbance of the core/shell plasmon, the spectra are blueshifted after being stored in hexane. The plasmon blueshift is particularly drastic in the PbS+$Cu_{2-x}S$ sample (**Figure S10e**), and there is no evidence that the PbS exciton remains in this sample.

References

1. Turo, M. J.; Macdonald, J. E., Crystal-Bound vs Surface-Bound Thiols on Nanocrystals. *ACS Nano* **2014,** *8* (10), 10205.
2. Bryks, W.; Wette, M.; Velez, N.; Hsu, S. W.; Tao, A. R., Supramolecular precursors for the synthesis of anisotropic Cu(2)S nanocrystals. *J Am Chem Soc* **2014,** *136* (17), 6175.
3. Lesnyak, V.; Brescia, R.; Messina, G. C.; Manna, L., Cu Vacancies Boost Cation Exchange Reactions in Copper Selenide Nanocrystals. *J Am Chem Soc* **2015,** *137* (29), 9315.
4. Sands, T. D.; Washburn, J.; Gronsky, R., High Resolution Observations of Copper Vacancy Ordering in Chalcocite (Cu_2S) and the Transformation to Djurleite ($Cu_{1.97\ to\ 1.94}S$). *Phys. Status Solidi. A* **1982,** *72*, 551.
5. Luther, J. M.; Jain, P. K.; Ewers, T.; Alivisatos, A. P., Localized surface plasmon resonances arising from free carriers in doped quantum dots. *Nat Mater* **2011,** *10* (5), 361.
6. Weidman, M. C.; Beck, M. E.; Hoffman, R. S.; Prins, F.; Tisdale, W. A., Monodisperse, Air-Stable PbS Nanocrystals via Precursor Stoichiometry Control. *ACS Nano* **2014,** *8* (6), 6363.